Composites Part B 116 (2017) 89–98

Contents lists available at ScienceDirect

Composites Part B

journal homepage: www.elsevier.com/locate/compositesb

Modeling framework for free edge effects in laminates under thermo-mechanical loading

M.S. Islam [a], P. Prabhakar [b, *]

[a] Department of Mechanical Engineering, Khulna University of Engineering & Technology, Bangladesh
[b] University of Wisconsin-Madison, Department of Civil & Environmental Engineering, WI 53706, United States

ARTICLE INFO

Article history:
Received 20 June 2016
Received in revised form
14 November 2016
Accepted 28 January 2017
Available online 21 February 2017

Keywords:
Free edge effect
Interface
Laminate
Finite element analysis

ABSTRACT

In this paper, a novel Quasi-2D (Q-2D) plane strain formulation for predicting interlaminar stresses in multi-directional laminates is developed and implemented within the finite element method framework. In particular, analyses of free edge stresses in composite laminates subjected to uniform axial and/or thermal loading are conducted. The Q-2D modeling approach presented here is validated by comparing the predicted interlaminar stresses with corresponding 3D models and previously published data. Computational time required for determining the interlaminar stresses using Q-2D model is approximately 30 times lower than the 3D analysis of the same laminate. Also, the Q-2D model is implemented within a commercially available software by modifying a 3D model to behave like a 2D model. This is particularly advantageous over developing an in-house finite element method code to capture the complex free edge stress states in multi-directional composites. Hence, the current framework can potentially be used as a computational tool for efficiently predicting the interlaminar stresses in different laminates subjected to thermo-mechanical loading, which can assist in determining interlaminar regions susceptible to free edge delamination.

1. Introduction

Interlaminar regions in polymer based layered carbon fiber composites are critical regions that are most susceptible to delamination under static and dynamic loading. Debonding or delamination is observed to be a significant failure mechanism in layered composites with considerable visible damage when subjected to load types like edge-wise and through-thickness compression, flexure, and dynamic impact. Delamination type failure is directly influenced by the strength and toughness of interlaminar regions. This is due to significant localized stresses that occur at the interlaminar regions, particularly at the free edges due to mismatch in property between plies, which commonly referred to as the “free edge effect” [1]. Hence, accurate determination of stress distribution near the free edges is very important due to their significant impact on delamination or transverse cracking in layered multi-directional laminates.

Stress state near the free edge is three dimensional in nature and classical lamination theory (CLT) is unable to determine these stresses accurately [1,2]. Therefore, various analytical and numerical approaches such as closed form analytical solutions, boundary layer theories, layer-wise theories, finite difference method and finite element method have been used by earlier researchers to calculate interlaminar stresses near the free edges. Puppo and Evensen [3] proposed the first analytical method to determine interlaminar stresses in a composite laminate. Pagano [4] developed a higher order plate theory to evaluate the interlaminar stresses, and Hsu and Herakovich [5] studied the free edge effects using perturbation and limiting free body approach for angle ply laminates. Tang [6], Davet and Destuynder [7], and Lin and Ko [8] studied similar problems using boundary layer theory. Pipes and Pagano [9] used an approximate elasticity solution, while Pagano [10] and Lekhnitskii and Fern [11] used variational principle to study the free edge effects in laminates. Yin [12,13] used a variational method that utilized Lekhnitskiis stress function for laminates under combined mechanical loading. Later, Yin [14] utilized the principle of complementary energy based on polynomial stress functions to evaluate the interlaminar stresses in laminates subjected non-uniform thermal loading. Andakhshideh and Tahani [15] used three dimensional multi-term extended Kantorovich method to investigate the interlaminar stresses near the free edges

* Corresponding author. Tel.: +16082657834.
E-mail address: pprabhakar4@wisc.edu (P. Prabhakar).

http://dx.doi.org/10.1016/j.compositesb.2017.01.072
1359-8368/

of general composite laminates under axial and shear loads. Amrutharaj et al. [16] investigated the free edge effects in composite laminates under uniaxial extension using the concept of fracture process zone. D'Ottavio et al. [17] conducted a comparative study of different plate theories for free edge effects in laminated plates and established that Layer-Wise (LW) theories are capable of capturing the free edge effects, while Equivalent Single Layer (ESL) theories fail. Even though the LW theories can capture the edge effects sufficiently well, they are computationally expensive [2] and the results often depend on the number of sublayers considered within each ply [18].

Pipes and Pagano [19] developed the first finite difference based numerical method to solve the two dimensional governing elasticity equations for calculating the interlaminar stresses of long symmetric laminate under uniform axial strain. Later, Atlus et al. [20] and Salamon [21] used three dimensional finite difference method to determine the interlaminar stresses in angle-ply laminates. Wang and Crossman [22,23] investigated edge effects in symmetric composite laminates subjected to uniform axial strain and thermal loading using finite element method. Herakovich et al. [24], Isakson and Levy [25], Rybicky [26], Kim and Hong [27], Icardi and Bertetto [28], Lessard et al. [29] and Yi and Hilton [30] also used finite element method to study free edge effects in laminates. Spilker and Chou [31] used a hybrid stress based finite element method, Lee and Chen [32] used a layer reduction technique, Robbins and Reddy [33] used a displacement based variable kinematic global local finite element method and Gaudenzi et al. [34] used a three dimensional multilayer higher order finite element method to study similar problems. Lorriot et al. [35] investigated the onset of delamination in carbon/epoxy laminates by developing a model based on stress criterion.

From the previous studies mentioned above, it is well established that free edge effects are dominant in multidirectional laminates and result in very high interlaminar stresses that prematurely initiate inter-layer delamination. Therefore, determining interfaces with very large interlaminar stresses is critical for the assessment of delamination driven failure. Interfaces most susceptible to delamination can be determined and strengthened accordingly during manufacturing to reduce their susceptibility to failure. Towards that, a Quasi-2D formulation within the finite element method (FEM) framework is established in this paper for determining delamination prone interlaminar regions in multidirectional laminates subjected to thermo-mechanical loading.

In the current paper, a variational formulation presented by Martin et al. [36] is extended for combined thermal and axial loading on multi-directional laminates, referred to as “Quasi-2D” (Q-2D) formulation. Q-2D formulation is implemented within the FEM framework for accurately determining stress distribution near the free edges for cross-ply ($[0/90]_s$) and quasi-isotropic ($[45/-45/90/0]_s$) laminates. A novel technique is developed in this paper for implementing the Q-2D model within the finite element framework, which involves modifying a thin slice of a 3D laminate to behave like a generalized 2D model by enforcing multi-point constraints. The approach presented in this paper is compared against corresponding 3D models and previously published data for establishing its validity and accuracy.

Other numerical approaches by earlier researchers have investigated the full 3D model to capture the free edge effects. For example, Icardi and Bertetto [28] used a 3D modeling approach with 20 noded quadratic isoparametric brick elements and 15 noded quadratic singular wedge elements for capturing the stress state at the free edges. Lessard et al. [29] also used 3D finite element method with 20 noded quadratic brick elements for the same. Raju and Crews [37] used a combined rectangular and polar mesh for their analysis, where the rectangular mesh was used to determine the stress distributions and polar mesh was used to investigate the stress singularities. But in the current paper, accurate stress states at the free edges are captured using a Quasi-2D reduced model, which takes about 30 times lesser computational time than a 3D model. Another key advantage of the Q-2D model is the easy implementation within any commercially available finite element software as opposed to the requirement of an in-house code.

This paper is divided into the following sections: Section 2 describes the mathematical formulation for the Q-2D, followed by the details of the implementation within the finite element framework in Section 3. Discussion of results from several case studies is presented in Section 4 followed by conclusions.

2. Mathematical formulation

Consider a laminate of length $2L$ and width $2b$, which consists of N layers (thickness h each) as shown in Fig. 1(a). Tensile load is applied on the edges at $\sum_{+L}$ and $\sum_{-L}$ along the x_1 direction, with free edges at $\sum_0$ and $\sum_{2b}$. A temperature change of ΔT occurs uniformly within the laminate.

The stress components are assumed to be independent of x_1 in regions sufficiently far from the loading surface [19,36], such that the displacement field $\{U\}$ can be defined as,

$$\begin{aligned} U_1(x_1,x_2,x_3) &= \tilde{U}_1(x_2,x_3) + \varepsilon_{11}x_1 \\ U_2(x_1,x_2,x_3) &= \tilde{U}_2(x_2,x_3) \\ U_3(x_1,x_2,x_3) &= \tilde{U}_3(x_2,x_3) \end{aligned} \tag{1}$$

where, ε_{11} is the uniform strain applied on the laminate along the x_1 direction. Displacement field $\{U\}$ and corresponding stress field $\{\sigma\}$ adhere to the following equations:

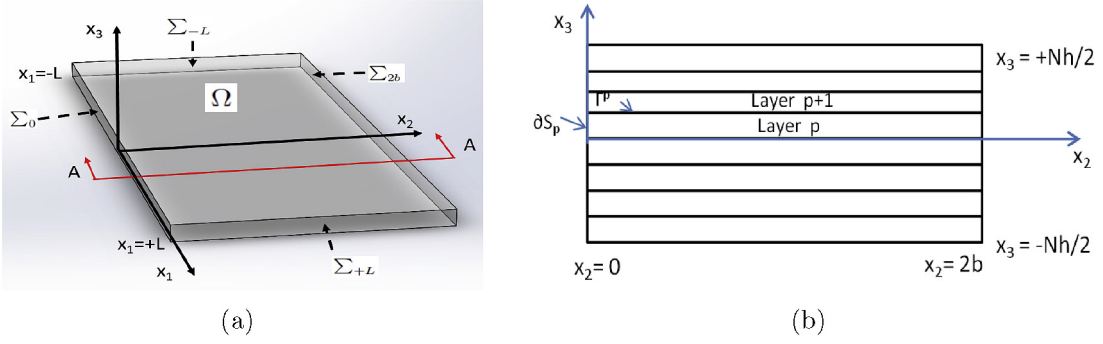

Fig. 1. (a)3D Laminate; (b) Cross-section of a 3D laminate.

$$\frac{\partial \sigma_{ij}}{\partial x_j} = 0, \sigma_{ij} = a_{ijkh}\epsilon^m_{kh}, \forall i = 1,2,3 \text{ within } \Omega, \tag{2}$$

$$\epsilon_{ij}(U) = \frac{1}{2}\left(\frac{\partial U_i}{\partial x_j} + \frac{\partial U_j}{\partial x_i}\right) \text{ within } \Omega; \tag{3}$$

$$[U_i] = 0, [\sigma_{ij} n_j] = 0 \text{ at the interfaces } \Gamma^p; [\sigma_{ij} n_j] = 0 \text{ on } \sum_{2b} \text{ and } \sum_{0} \tag{4}$$

$$[\sigma_{ij} n_j] = F_i \text{ on } \sum_{+L} \text{ and } \sum_{N\frac{h}{2}}; [\sigma_{ij} n_j] = -F_i \text{ on } \sum_{-L} \text{ and } \sum_{-N\frac{h}{2}} \tag{5}$$

Introducing a trial field V with $\varepsilon_{11} = 0$ and averaging equation (2) over the domain gives,

$$\int_\Omega \frac{\partial \sigma_{ij}}{\partial x_j} V_i d\Omega = 0, \forall V_i \text{ with i} = 1,\ 2,\ 3. \tag{6}$$

Applying divergence theorem to the above equation yields,

$$\int_\Omega \sigma_{ij} \frac{\partial V_i}{\partial x_j} d\Omega = \int_{\sum_{+L}} F_i V_i dS - \int_{\sum_{-L}} F_i V_i dS \tag{7}$$

Since, V_i does not depend on x_1:

$$\int_\Omega \sigma_{il} \frac{\partial V_i}{\partial x_l} d\Omega = 0, \forall V_i \text{ with } l = 2,3. \tag{8}$$

Using $\sigma_{ij} = a_{ijkh}\epsilon^m_{kh}$ yields,

$$\int_\Omega a_{ilkh}\left(\frac{\partial U_k}{\partial x_h} - \alpha_{kh}\Delta T\right)\frac{\partial V_i}{\partial x_l} d\Omega = 0, \forall V_i \text{ for i, k, h} = 1,\ 2,\ 3; \text{ l} = 2,\ 3 \tag{9}$$

where, $\{\varepsilon^m\} = \{\varepsilon\} - \{\alpha\}\Delta T$.

Substituting the displacement field assumption given in equation (1) and (9) gives,

$$\int_\Omega a_{ilkh}\left(\frac{\partial \tilde{U}_k}{\partial x_h} - \alpha_{kh}\Delta T\right)\frac{\partial V_i}{\partial x_l} dx_1 dx_2 dx_3 + \varepsilon_{11}\int_\Omega a_{il11}\frac{\partial V_i}{\partial x_l} dx_1 dx_2 dx_3 = 0 \tag{10}$$

Splitting the volume integral into a surface integral in the plane of the cross-section (x_2, x_3) and line integral along the x_1 direction yields,

$$\begin{aligned}
&\int_{-L}^{+L} dx_1 \int_S a_{ilk\beta}\left(\frac{\partial \tilde{U}_k}{\partial x_\beta} - \alpha_{k\beta}\Delta T\right)\frac{\partial V_i}{\partial x_l} dx_2 dx_3 \\
&- \int_{-L}^{+L} dx_1 \int_S a_{ilk1}\alpha_{k1}\Delta T \frac{\partial V_i}{\partial x_l} dx_2 dx_3 \\
&+ \varepsilon_{11}\int_{-L}^{+L} dx_1 \int_S a_{il11}\frac{\partial V_i}{\partial x_l} dx_2 dx_3 \\
&= 0,
\end{aligned} \tag{11}$$

with $l, \beta = 2,3$.

$$\begin{aligned}
&\int_S a_{ilk\beta}\left(\frac{\partial \tilde{U}_k}{\partial x_\beta} - \alpha_{k\beta}\Delta T\right)\frac{\partial V_i}{\partial x_l} dx_2 dx_3 \\
&= \Delta T \int_S a_{ilk1}\alpha_{k1}\frac{\partial V_i}{\partial x_l} dx_2 dx_3 - \varepsilon_{11}\int_S a_{il11}\frac{\partial V_i}{\partial x_l} dx_2 dx_3
\end{aligned} \tag{12}$$

Applying divergence theorem on the right hand side,

$$\begin{aligned}
&\int_{S^p} a_{ilk\beta}\left(\frac{\partial \tilde{U}_k}{\partial x_\beta} - \alpha_{k\beta}\Delta T\right)\frac{\partial V_i}{\partial x_l} dx_2 dx_3 \\
&= \Delta T \int_{\partial S} a_{ilk1}\alpha_{k1} V_i n_l ds - \varepsilon_{11}\int_{\partial S} a_{il11} V_i n_l ds
\end{aligned} \tag{13}$$

where, "s" represents a coordinate that denotes the boundary ∂S, starting at the origin of the $x_2 - x_3$ axes for the region S and traversing in the counter-clockwise direction. Therefore, "s" is either "x_2" or "x_3" depending on the edge on the boundary being traversed.

The above equation is modified to account for the through-thickness layers with different orientations in a multi-directional laminate as:

$$\begin{aligned}
&\sum_{p=1}^{N} \int_{S^p} a^p_{ilk\beta}\left(\frac{\partial \tilde{U}^p_k}{\partial x_\beta} - \alpha^p_{k\beta}\Delta T\right)\frac{\partial V^p_i}{\partial x_l} dx_2 dx_3 \\
&= \Delta T \sum_{p=1}^{N} \int_{\partial S^p} a^p_{ilk1}\alpha^p_{k1} V^p_i n^p_l ds - \varepsilon_{11}\sum_{p=1}^{N} \int_{\partial S^p} a^p_{il11} V^p_i n^p_l ds
\end{aligned} \tag{14}$$

Upon expanding the right hand side of equation (14), contributions of the vertical edges is given by,

$$\Delta T\sum_{p=1}^{N}\left(\int_{-Nh/2+(p-1)h}^{Nh/2+ph} a_{i2k1}^{p}\alpha_{k1}^{p}V_i^{p}(2b,x_3)dx_3 - \int_{-Nh/2+(p-1)h}^{Nh/2+ph} a_{i2k1}^{p}\alpha_{k1}^{p}V_i^{p}(0,x_3)dx_3\right) - \varepsilon_{11}\sum_{p=1}^{N}\left(\int_{-Nh/2+(p-1)h}^{Nh/2+ph} a_{i211}^{p}V_i^{p}(2b,x_3)dx_3 - \int_{-Nh/2+(p-1)h}^{Nh/2+ph} a_{i211}^{p}V_i^{p}(0,x_3)dx_3\right) \quad (15)$$

Similarly, contribution of each interface is,

$$\Delta T\sum_{p=1}^{N-1}\left(-\int_{0}^{2b}\left(a_{i3k1}^{p+1}\alpha_{k1}^{p+1}-a_{i3k1}^{p}\alpha_{k1}^{p}\right)V_i^{p}\left(x_2,N\frac{h}{2}+ph\right)dx_2\right) - \varepsilon_{11}\sum_{p=1}^{N-1}\left(-\int_{0}^{2b}\left(a_{i311}^{p+1}-a_{i311}^{p}\right)V_i^{p}\left(x_2,N\frac{h}{2}+ph\right)dx_2\right) \quad (16)$$

Contribution of top and bottom edges is,

$$\Delta T\left(-\int_{0}^{2b} a_{i3k1}^{1}\alpha_{k1}^{1}V_i^{1}\left(x_2,-N\frac{h}{2}\right)dx_2 + \int_{0}^{2b} a_{i3k1}^{N}\alpha_{k1}^{N}V_i^{N}\left(x_2,N\frac{h}{2}\right)dx_2\right) - \varepsilon_{11}\left(-\int_{0}^{2b} a_{i311}^{1}V_i^{1}\left(x_2,-N\frac{h}{2}\right)dx_2 + \int_{0}^{2b} a_{i311}^{N}V_i^{N}\left(x_2,N\frac{h}{2}\right)dx_2\right) \quad (17)$$

Equation (14) is a generalized 2D formulation with displacement fields in the x_1, x_2 and x_3 directions. Inputs to the above formulation are the fourth order elasticity tensor of each layer of the laminate within the linear elastic limit, coefficient of thermal expansions, applied external strain and change in temperature. The effective loads calculated for a multi-directional laminate are applied to the 2D generalized representation of the laminate in the FEM model explained in the following section.

3. Implementation of the Quasi-2D formulation

The above formulation can be implemented in several ways within finite element method. However, a novel technique is developed in this paper by modifying a thin slice of a 3D model to behave like a generalized 2D model. A 3D model with a small thickness (1 mm in this case) along the x_1-direction is considered as shown in Fig. 2(a) with only one element in the x_1-direction. Multi-point constraints are applied between the front and back faces of the model such that the displacement fields are independent of the x_1-direction. For illustration, consider a nodal point 'm' on the front surface and a corresponding nodal point on the back surface as shown in Fig. 2(b). These two points (m and n) are tied together such that the displacements U_1, U_2 and U_3 are identical for the nodal pair. Similarly, all the nodal points on the front surface are tied with their corresponding points on the back surface. Since, only one element exists in the x_1-direction, the constraint enforces the requirement of displacement fields being independent of that direction, that is, U_1, U_2 and U_3 are now functions of x_2 and x_3 only. This simulates the left hand side of equation (14). The external loads established by the right hand side of equation (14) are applied on the edges and interfaces between the layers of the model in the $x_2 - x_3$ plane.

Eight noded linear hexahedral elements (C3D8 in ABAQUS notation [38]) are used to mesh the Q-2D model as shown in Fig. 3(a). Very fine mesh is used near the interfaces and free edges to sufficiently capture the stress singularities within these regions. The element size in these regions is 1 μm and the total number of elements in a single ply for $[45/-45/90/0]_s$ laminate is 5856. The interlaminar stresses near the free edges and interfaces appear to vary with the size of the elements. Hence, mesh sensitivity analysis is performed to determine the element sizes that minimize the dependency of stress profile on the mesh. Element sizes are varied linearly from a very fine mesh at the free edges and interfaces to course mesh away in the interior regions of the model in the $x_2 - x_3$ plane. This mesh refinement is conducted until no significant change in the interlaminar stress profile is observed. However, only one element is used along the x_1 direction to enforce multi-point constraint described above. Due to relatively large number of nodes on the front and back faces in the $x_2 - x_3$ plane, enforcing multi-point constraints manually is cumbersome. Hence, a script to assign the multi-point constraints on a generic laminate is developed, which is described in detail in the following paragraph.

A python™ script is written that reads an ABAQUS input file and includes the multi-point constraints at the appropriate sections of

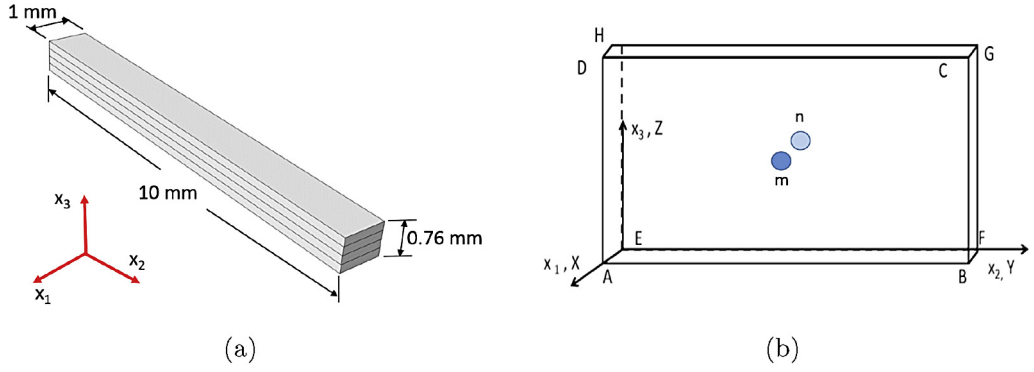

Fig. 2. 3D slice of a laminate.

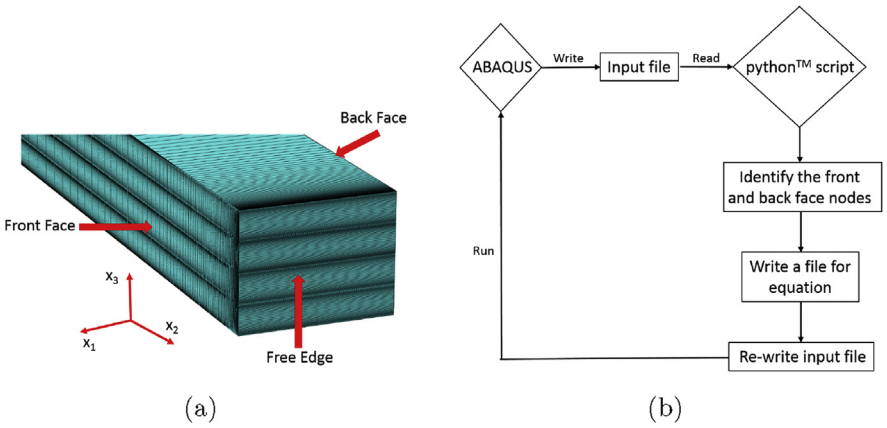

Fig. 3. (a) Typical mesh in the Q-2D model; (b) Working principle of python™ script.

the file. Working procedure of the python™ script is shown in Fig. 3(b). The input file obtained from ABAQUS without constraints is read by the python™ script, which identifies the nodal pairs between the front and back faces. The script then writes the constraint equations for each nodal pair in a different file. Then, the main input file is re-written with the equations file called using "*INCLUDE". Fig. 4(a) shows a snapshot of the re-written input file which includes the equation file as an "input", and Fig. 4(b) shows a snapshot of the equation file with constraint equations written.

For illustration, Fig. 5 shows the boundary conditions for $[45/-45/90/0]_s$ laminate subjected to an uniform axial strain, which is derived from Equation (14). As mentioned in the previous section, key inputs to the Q-2D model are the 4th order elasticity tensor of individual layers and the applied strain. Effective loads that depend on the elastic constants are applied as pressure along the normal direction and surface tractions parallel to the edges as shown in Fig. 5. Here, $\overrightarrow{x_1}$, $\overrightarrow{x_2}$ and $\overrightarrow{x_3}$ indicate the directions of the applied effective loads on each layer. The loads corresponding to $\overrightarrow{x_3}$ direction are not shown in the figure since the associated elastic constants are equal to zero in the current example. Accordingly, the effective interface loads are applied along the interfaces between the layers.

For several cases considered in this paper, full 3D models are also analyzed to validate the results from the corresponding Q-2D models. Towards that, only $1/8^{th}$ of a 3D model is analyzed due to symmetry as shown in Fig. 6. Linear hexahedral (C3D8 as mentioned before) elements are used with a minimum element size at the interfaces and free edges equal to 1 μm. For example, this yields a total number of elements in a single ply for $[45/-45/90/0]_s$ laminate equal to 79696. Mesh sensitivity analysis for the 3D models similar to Q-2D model is performed as well.

4. Results and discussions

The Q-2D model is applied to several laminates subjected to three main types of loading: uniform axial extension (Section 4.1), uniform thermal loading (Section 4.2) and combined axial and thermal loading (Section 4.3). Results are compared with published data (where available) and 3D model results to establish the reliability of the current modeling approach.

4.1. Case 1: axial loading

In this section, $[0/90]_s$ and $[45/-45/90/0]_s$ laminates subjected to a uniform axial (x_1-direction) strain are considered. The following material properties are used: $E_{11} = 137.9$ GPa, $E_{22} = E_{33} = 14.48$ GPa, $G_{12} = G_{13} = G_{23} = 5.86$ GPa and $\nu_{12} = \nu_{13} = \nu_{23} = 0.21$, which correspond to a high modulus graphite/epoxy laminate [18]. The $[0/90]_s$ cross-ply laminate subjected to a uniform axial (x_1-direction) strain has been previously investigated by Zhang et al. [1], Tahani and Nosier [2], Nguyen and Caron [18], Wang and Crossman [23], Carreira et al. [39] and Zhen et al. [40]. Fig. 7 shows the comparison of interlaminar stress distribution at the 0/90 interface of $[0/90]_s$ laminate subjected to a uniform axial strain with few previously published articles. Even though, Fig. 7(a) shows that the present model predicts slightly higher interlaminar normal stress at the edges compared to previous studies, the behavior is identical. The shear stress (σ_{23}) distribution is comparable to other models (Fig. 7(b)).

For $[45/-45/90/0]_s$ laminate, seldom results are found in the literature to compare the results from the current Q-2D model. Hence, a full 3D model is analyzed and the results from the Q-2D model is compared with the corresponding 3D model. Fig. 8 shows

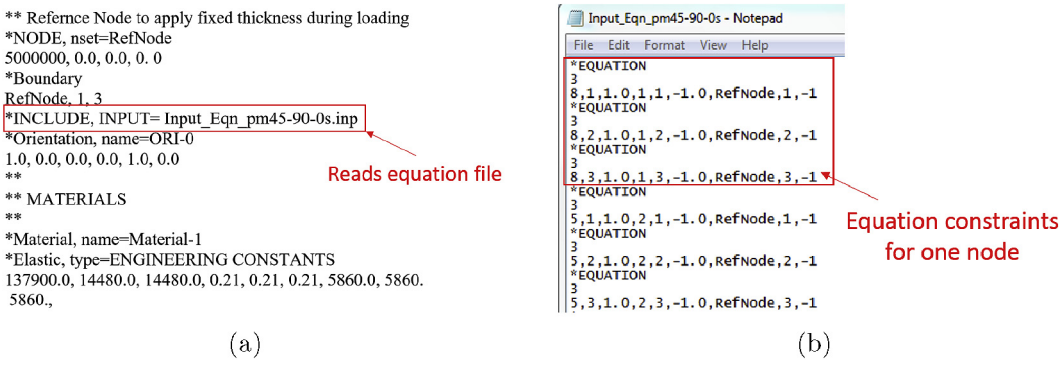

Fig. 4. Snapshot of (a) input file and (b) equation file.

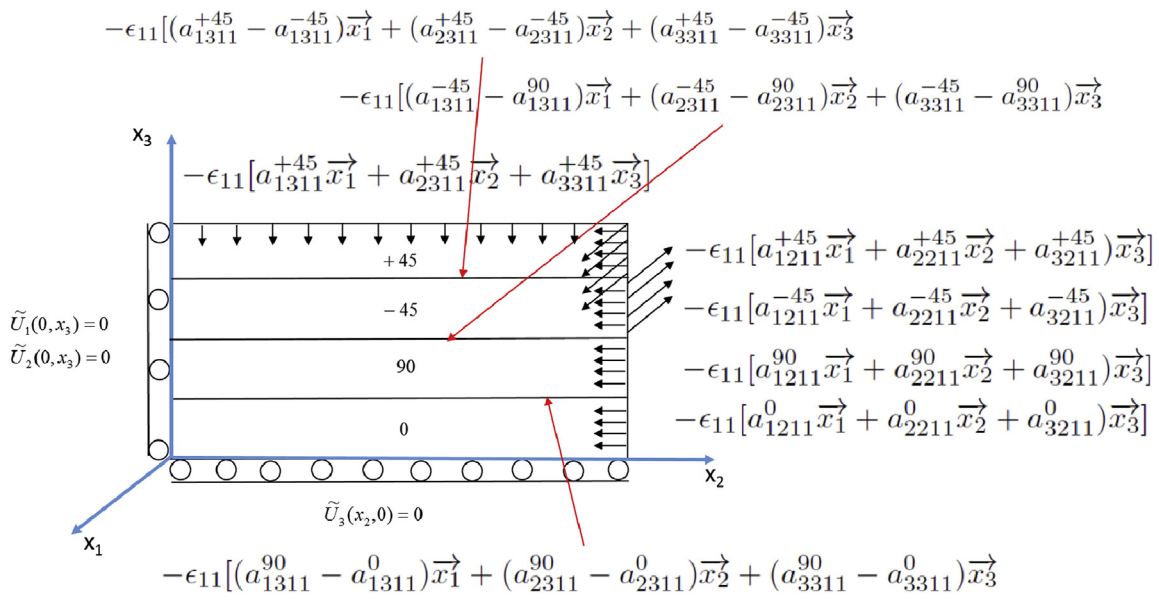

Fig. 5. Boundary conditions for uniaxial extension.

the comparison of Q-2D and 3D models at different interfaces, which shows an excellent agreement between these two models.

4.2. Case 2: thermal loading

In this section, $[0/90]_s$ and $[45/-45/90/0]_s$ laminates subjected to a uniform temperature change ΔT throughout the modeling domain are considered. For direct comparison with previously published results, the following material properties are used: $E_{11}=137.9$ GPa, $E_{22}=E_{33}=14.48$ GPa, $G_{12}=G_{13}=G_{23}=5.86$ GPa, $\nu_{12}=\nu_{13}=\nu_{23}=0.21$, $\alpha_1=0.36\times10^{-6}\ ^\circ C^{-1}$ and $\alpha_2=\alpha_3=28.8\times10^{-6}\ ^\circ C^{-1}$. Fig. 9 shows the distribution of σ_{33} (Fig. 9(a)) and σ_{23} (Fig. 9(b)) for $\Delta T=1\ ^\circ C$. It is observed that the current results are in excellent agreement with those determined by previous researchers [2,14,18].

Fig. 10 shows the distribution of interlaminar stresses for $[45/-45/90/0]_s$ laminate subjected to a uniform temperature change $\Delta T=1\ ^\circ C$ along the +45/-45 (Fig. 10(a)), −45/90 (Fig. 10(b)) and 90/0 interfaces (Fig. 10(c)). It is observed that the current results are in good agreement with the corresponding 3D model results.

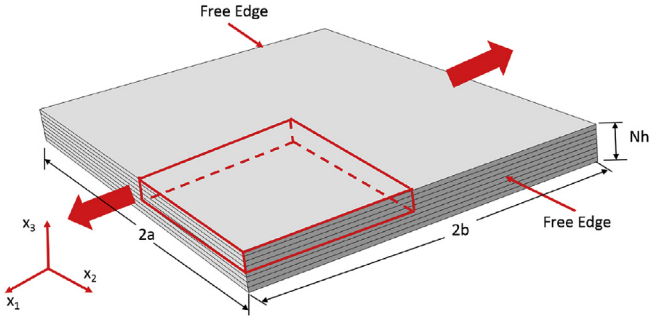

Fig. 6. 3D model.

4.3. Case 3: combined axial and thermal loading

In this section, $[0/90]_s$ and $[45/-45/90/0]_s$ laminates subjected to a uniform axial strain ($\varepsilon_{11}=0.01$) and uniform temperature change ($\Delta T=1\ ^\circ C$) are considered. The material properties used here are the same as those mentioned in Section 4.2. Fig. 11 and 12 show the distribution of interlaminar stresses for $[0/90]_s$ and $[45/-45/90/0]_s$ laminates subjected to $\varepsilon_{11}=0.01$ and $\Delta T=25\ ^\circ C$.

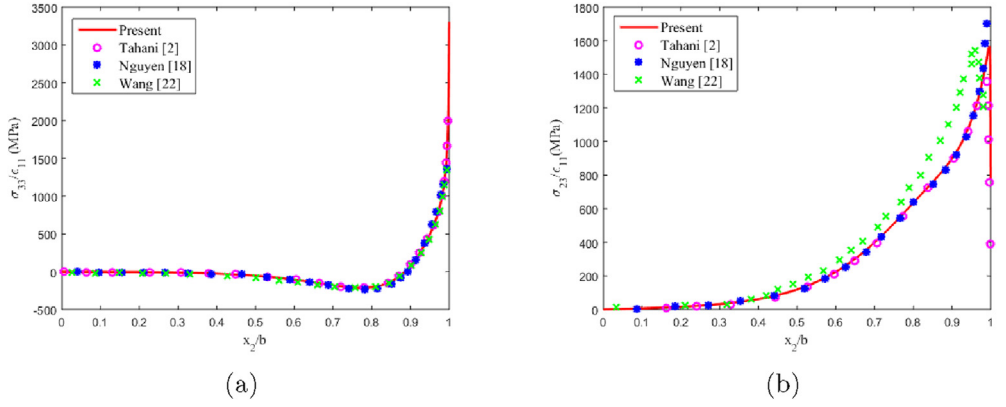

Fig. 7. Distribution of interlaminar stresses along the 0/90 interface of [0/90]s laminate subjected to a uniform axial extension (a) normal stress σ_{33} and (b) shear stress σ_{23}.

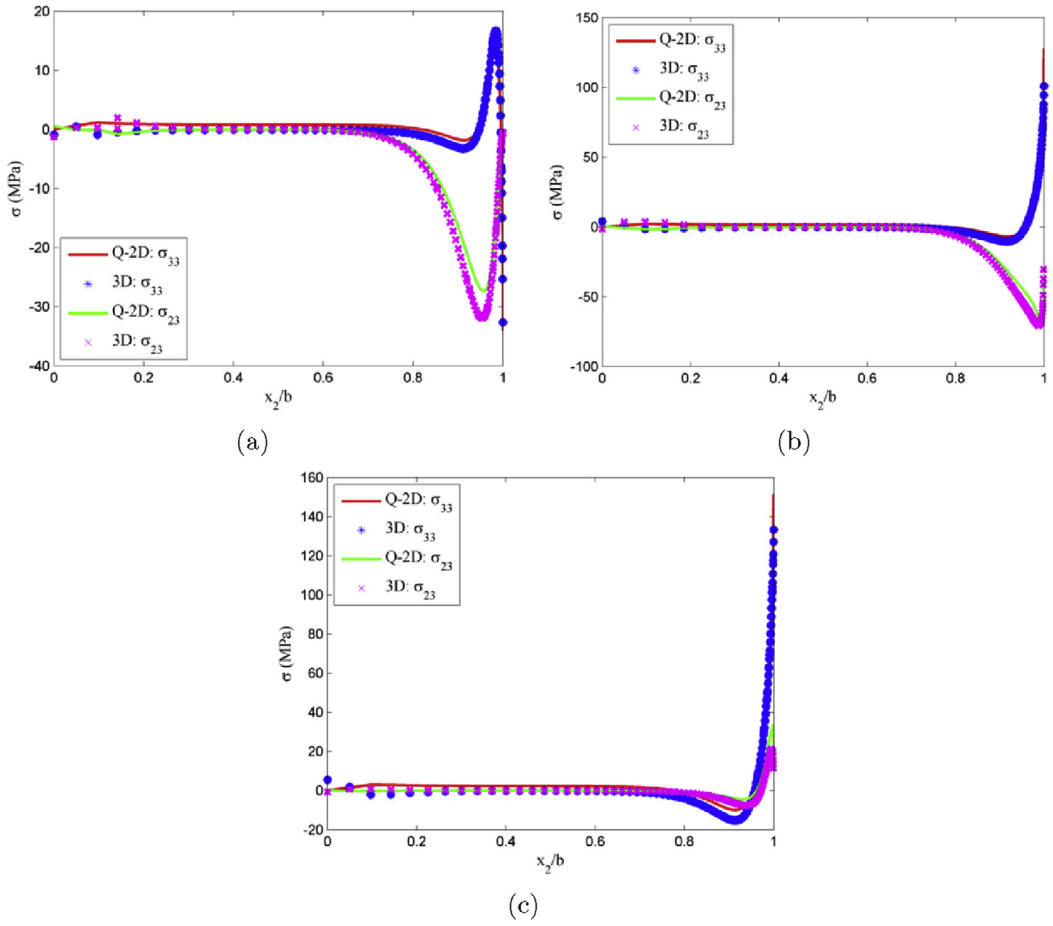

Fig. 8. Distribution of interlaminar stress of $[45/-45/90/0]_s$ laminate subjected to uniform axial extension along (a) 45/-45, (b) −45/90 and (c) 90/0 interface.

These results are compared with their corresponding 3D models and is observed (Fig. 11 and 12) that the current results are in excellent agreement with the 3D results.

4.4. Comparison of Q-2D model with 3-D model

The Q-2D modeling framework developed in this paper utilizes a fairly straight forward derivation and an easy implementation within existing finite element method softwares. It is also highly efficient with respect to computational cost when compared to the 3D counterpart models. A direct comparison of the efficiency of Q-2D models with 3D models is performed due to insufficient data found in the literature about the computational time, processor used, etc. for other published methods. Table 1 shows a comparison of the computational time required by the Q-2D and 3D models of $[45/-45/90/0]_s$ laminate (it takes approximately the same time for all loading cases). The total computational time required by the Q-2D model is approximately 2 min and that for the 3D model is approximately 60 min using the same Intel® Core™ i7-3540 M 3.00 GHz CPU. It should be noted that although 60 min seems like a reasonable time for a 3D model, it is for an 8 layer laminate ($[45/-45/90/0]_s$) only. The time required will scale up with increased number of layers in the case of thicker laminates (for example 48 layers). Further, such a modeling approach will drastically reduce the computational cost associated with optimization problems, where large number of simulations are required. Hence, the Q-2D model can save the computational time significantly while predicting the interlaminar stress distribution with high level of accuracy as compared to 3D models.

5. Conclusions

In this study, a Quasi-2D modeling approach to determine free edge effects in laminated composites was developed and implemented within the finite element method framework. The interlaminar stresses determined using this approach are comparable to that of a full 3D model. Also, the accuracy and effectiveness of the current Q-2D model is validated with previously published results. In particular, free edge effects in $[0/90]_s$ and $[45/-45/90/0]_s$ laminates subjected to uniform axial extension, uniform temperature distribution and combined axial-thermal loading were investigated with the Q-2D modeling approach. Primarily, normal (σ_{33}) and shear (σ_{23}) stresses at the interlaminar regions were examined due to their propensity to create delaminations. The Q-2D model was capable of predicting the interlaminar stresses for different laminates subjected to uniform axial and/or thermal loading efficiently with high level of accuracy. The current formulation includes thermal and uni-axial loading cases, however, further development is needed for capturing the effects of inhomogeneous material/geometry or fully multi-axial loading. Key outcomes of the research presented in this paper are as follows:

- The computational time required to solve for the interlaminar stresses in multi-directional laminates using Q-2D model is approximately 30 times lower than the corresponding 3D model of the same laminate.

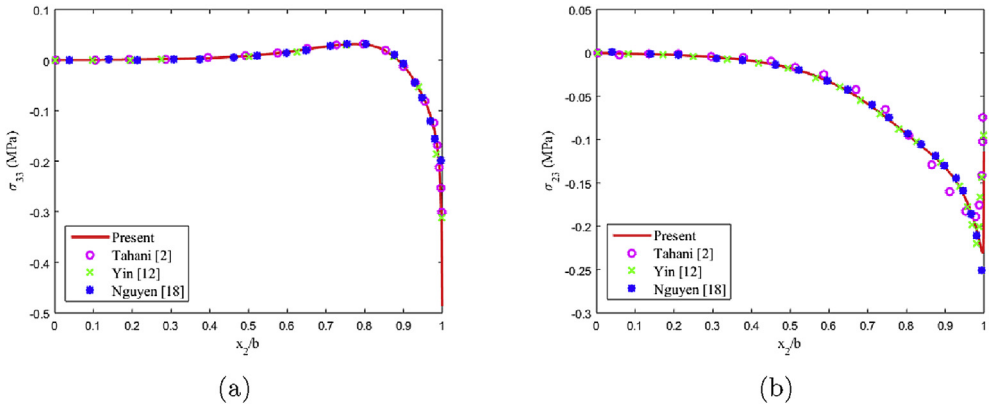

Fig. 9. Distribution of interlaminar stresses along the 0/90 interface of [0/90]s laminate due to a temperature change $\Delta T = 1^{\circ}C$ (a) normal stress σ_{33} and (b) shear stress σ_{23}.

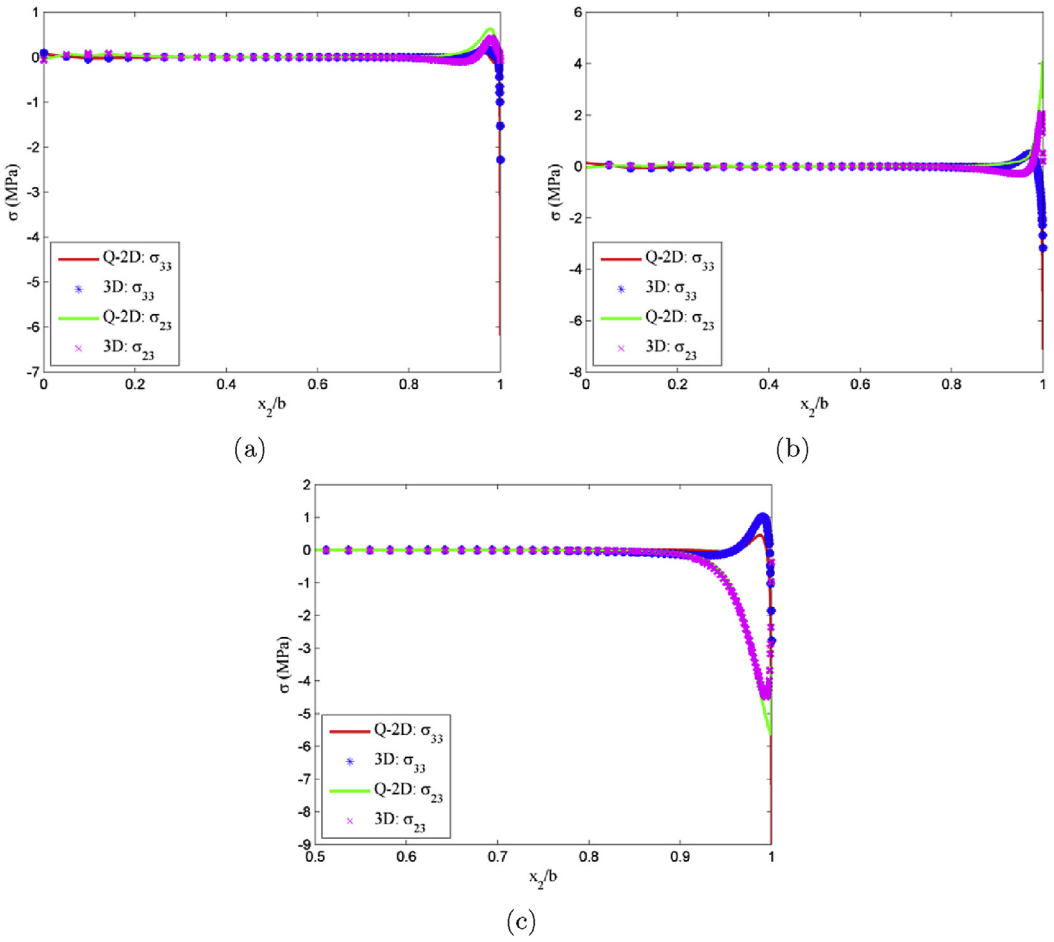

Fig. 10. Distribution of interlaminar stress of $[45/-45/90/0]_s$ laminate due to a temperature change $\Delta T = 25^{\circ}C$ (a) 45/-45, (b) −45/90 and (c) 90/0 interface.

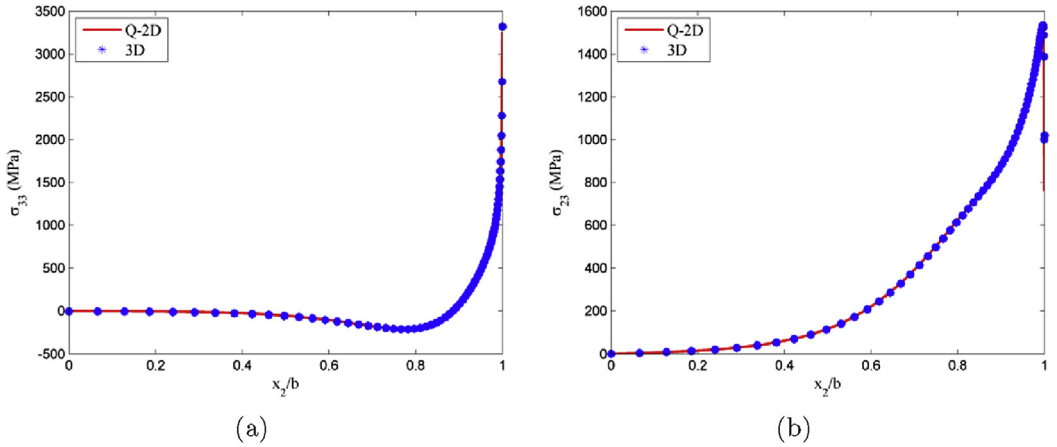

Fig. 11. Distribution of interlaminar stress along the 0/90 interface of $[0/90]_s$ laminate subjected to $\varepsilon_{11} = 0.01$ and $\Delta T = 25\ ^\circ C$ (a) normal stress σ_{33} and (b) shear stress σ_{23}.

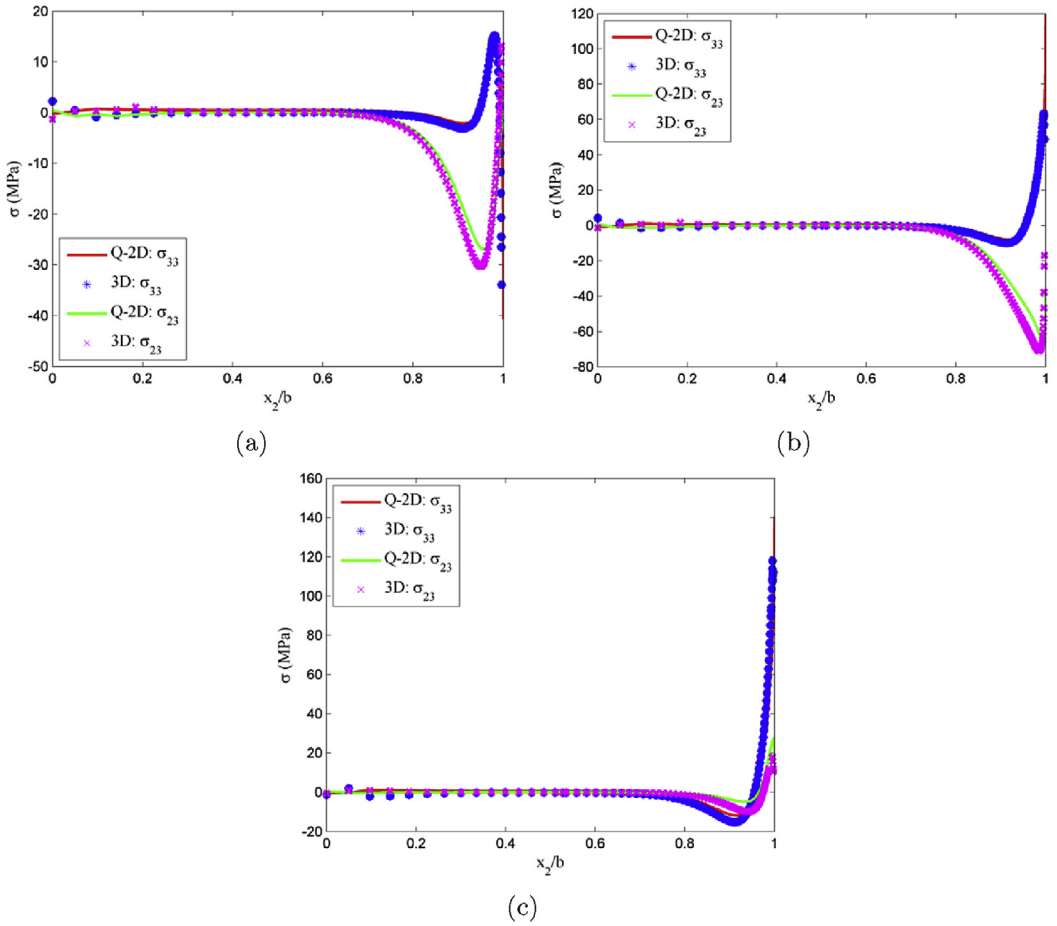

Fig. 12. Distribution of interlaminar stress of $[45/-45/90/0]_s$ laminate subjected to $\varepsilon_{11} = 0.01$ and $\Delta T = 25\ ^\circ C$ along (a) 45/-45, (b) −45/90 and (c) 90/0 interface.

- Existing finite element framework within a commercially available software is used to determine interlaminar stresses by modifying a 3D model to behave like a 2D model. This is particularly advantageous since developing an in-house FEM code can be avoided for determining complex stress states at free edges of multi-directional laminates.

Table 1
Comparison of Q-2D and 3D model.

Model	No. of Elements	Approximate Time (min)
Q-2D	23424	2
3D	318786	60

Acknowledgements

The authors would like to acknowledge Dr. David Stargel for their support through the AFOSR Young Investigator Program (Grant No.: FA9550-15-1-0216) to conduct this research.

References

[1] Zhang D, Ye J, Sheng HY. Free-edge and ply cracking effect in cross-ply laminated composites under uniform extension and thermal loading. Compos Struct 2006;76(4):314–25.
[2] Tahani M, Nosier A. Free edge stress analysis of general cross-ply composite laminates under extension and thermal loading. Compos Struct 2003;60(1):91–103.
[3] Puppo AH, Evensen HA. Interlaminar shear in laminated composites under generalized plane stress. J Compos Mater 1970;4(2):204–20.
[4] Pagano NJ. On the calculation of interlaminar normal stress in composite laminate. J Compos Mater 1974;8(1):65–81.
[5] Hsu PW, Herakovich CT. Edge effects in angle-ply composite laminates. J Compos Mater 1977;11(4):422–8.
[6] Tang S. A boundary layer theory-part i: laminated composites in plane stress. J Compos Mater 1975;9(1):33–41.
[7] Davet JL, Destuynder Ph. Free-edge stress concentration in composite laminates: a boundary layer approach. Comput methods Appl Mech Eng 1986;59(2):129–40.
[8] Lin CC, Ko CC. Method for calculating the interlaminar stresses in symmetric laminates containing a circular hole. AIAA J 1992;30(1):197–204.
[9] Pipes RB, Pagano NJ. Interlaminar stresses in composite laminatesan approximate elasticity solution. J Appl Mech 1974;41(3):668–72.
[10] Pagano NJ. Stress fields in composite laminates. Int J Solids Struct 1978;14(5):385–400.
[11] Leknitskii SG, Fern P. Theory of elasticity of an anisotropic elastic body. Holden-Day; 1963.
[12] Yin WL. Free-edge effects in anisotropic laminates under extension, bending and twisting, part i: a stress-function-based variational approach. J Appl Mech 1994a;61(2):410–5.
[13] Yin WL. Free-edge effects in anisotropic laminates under extension, bending, and twisting, part ii: eigenfunction analysis and the results for symmetric laminates. J Appl Mech 1994b;61(2):416–21.
[14] Yin WL. The effect of temperature gradient on the free-edge interlaminar stresses in multi-layered structures. J Compos Mater 1997;31(24):2460–77.
[15] Andakhshideh A, Tahani M. Interlaminar stresses in general thick rectangular laminated plates under in-plane loads. Compos Part B Eng 2013;47:58–69.
[16] Amrutharaj GS, Lam KY, Cotterell B. Delaminations at the free edge of a composite laminate. Compos Part B Eng 1996;27(5):475–83.
[17] DOttavio M, Vidal P, Valot E, Polit O. Assessment of plate theories for free-edge effects. Compos Part B Eng 2013;48:111–21.
[18] Nguyen VT, Caron JF. Finite element analysis of free-edge stresses in composite laminates under mechanical an thermal loading. Compos Sci Technol 2009;69(1):40–9.
[19] Pipes RB, Pagano NJ. Interlaminar stresses in composite laminates under uniform axial extension. J Compos Mater 1970;4(4):538–48.
[20] Altus E, Rotem A, Shmueli M. Free edge effect in angle ply laminates- a new three dimensional finite difference solution. J Compos Mater 1980;14:21–30.
[21] Salamon NJ. Interlaminar stressess in a layered composite laminate in bending. Fibre Sci Technol 1978;11(4):305–17.
[22] Wang ASD, Crossman FW. Some new results on edge effect in symmetric composite laminates. J Compos Mater 1977a;11(1):92–106.
[23] Wang ASD, Crossman FW. Edge effects on thermally induced stresses in composite laminates. J Compos Mater 1977b;11(3):300–12.
[24] C.T. Herakovich, G.D. Renieri, and H.F. Brinson. Finite element analysis of mechanical and thermal edge effects in composite laminates. In army symposium on solid mechanics, composite materials: the influence of mechanics of failure on design, Cape Cod (USA), pages 237–248, 1976.
[25] Isakson G, Levy A. Finite-element analysis of interlaminar shear in fibrous composites. J Compos Mater 1971;5(2):273–6.
[26] Rybicki EF. Approximate three-dimensional solutions for symmetric laminates under inplane loading. J Compos Mater 1971;5(3):354–60.
[27] Kim JY, Hong CS. Three-dimensional finite element analysis of interlaminar stresses in thick composite laminates. Comput Struct 1991;40(6):1395–404.
[28] Icardi U, Bertetto AM. An evaluation of the influence of geometry and of material properties at free edges and at corners of composite laminates. Comput Struct 1995;57(4):555–71.
[29] Lessard LB, Schmidt AS, Shokrieh MM. Three-dimensional stress analysis of free-edge effects in a simple composite cross-ply laminate. Int J Solids Struct 1996;33(15):2243–59.
[30] Yi S, Hilton HH. Finite element analysis of free edge stresses in non-linear viscoelastic composites under uniaxial extension, bending and twisting loadings. Int J Numer methods Eng 1997;40(22):4225–38.
[31] Spilker RL, Chou SC. Edge effects in symmetric composite laminates- importance of satisfying the traction-free-edge condition. J Compos Mater 1980;14:2–20.
[32] Lee CY, Chen JM. Interlaminar shear stress analysis of composite laminate with layer reduction technique. Int J Numer methods Eng 1996;39(5):847–65.
[33] Robbins DH, Reddy JN. Variable kinematic modelling of laminated composite plates. Int J Numer Methods Eng 1996;39(13):2283–317.
[34] Gaudenzi P, Mannini A, Carbonaro R. Multi-layer higher-order finite elements for the analysis of free-edge stresses in composite laminates. Int J Numer methods Eng 1998;41(5):851–73.
[35] Lorriot T, Marion G, Harry R, Wargnier H. Onset of free-edge delamination in composite laminates under tensile loading. Compos Part B Eng 2003;34(5):459–71.
[36] Martin E, Leguillon D, Carrère N. A twofold strength and toughness criterion for the onset of free-edge shear delamination in angle-ply laminates. Int J Solids Struct 2010;47(9):1297–305.
[37] Raju IS, Crews JH. Interlaminar stress singularities at a straight free edge in composite laminates. Comput Struct 1981;14(1):21–8.
[38] Prabhakar P, Waas AM. Micromechanical modeling to determine the compressive strength and failure mode interaction of multidirectional laminates. Compos Part A Appl Sci Manuf 2013;50:11–21.
[39] Carreira RP, Caron JF, Diaz AD. Model of multilayered materials for interface stresses estimation and validation by finite element calculations. Mech Mater 2002;34(4):217–30.
[40] Lo SH, Zhen W, Cheung YK, Wanji C. An enhanced global–local higher-order theory for the free edge effect in laminates. Compos Struct 2007;81(4):499–510.